

Numerical determination of crack width for reinforced concrete deep beams

Aydin Demir* and Naci Caglar^a

Department of Civil Engineering, Faculty of Engineering, Sakarya University,
Esentepe Campus, 54050 Serdivan, Sakarya, Republic of Turkey

(Received October 17, 2019, Revised February 12, 2020, Accepted February 20, 2020)

Abstract. In the study, a new, simple and alternative formula is proposed to calculate numerically crack widths of concrete on a finite element (FE) model. By considering more general tension softening behavior of concrete, the proposed expression is derived irrespective of any tension softening model given in the literature or design codes. The test results of six reinforced concrete (RC) deep beams having different geometrical and material properties selected from a recent existing experimental study of the authors are used to verify the accuracy and reliability of the proposed formula and the created numerical FE models of the specimens. Moreover, the crack width results obtained from the FE models are compared with the test results to see the performance of the proposed formula. The results of the study demonstrate that the proposed formula gives very accurate results in a comparison with the test results. The ratios of errors on the results stay commonly at an acceptable level as well. Consequently, the proposed formula is quite simple, unique, and robust to determine crack widths of RC deep beams on an FE model.

Keywords: crack width formula; numerical determination of crack width; tension softening; concrete damage plasticity; reinforced concrete deep beam

1. Introduction

The scatter and width of cracks are major parameters to determine the serviceability behavior of reinforced concrete (RC) structures. The initiation and propagation of cracks play a very important role in the determination of nonlinear behavior of RC members. Thus, the damage and failure mechanism of structures depends on the behavior of their cracked members. Moreover, the crack directions change according to loading history and so the behavior of a structure depends on the behavior of the cracks existing on its structural members (Bazant and Oh 1983, Vecchio and Collins 1986, Rots 1988). Therefore, monitoring the initiation, propagation, and width of cracks is essential to observe the strength and serviceability behavior of RC structures.

The cracking and serviceability of RC members are generally investigated via experimental studies. Many empirical design recommendations are proposed to ensure a safe design of structures under different loading conditions according to the findings obtained in those studies. While conducting an experimental study is one of the most reliable, accurate and globally accepted techniques to investigate the cracking behavior of RC members, it has some disadvantages in terms of inconvenience, time, labor, and budget. However, conducting a numerical study including a reliable finite element (FE) modeling technique and appropriate constitutive material models is an

alternative, accurate, and robust tool to simulate the nonlinear behavior of RC members. Therefore, the FE method is one of the widely preferred techniques by researchers for their scientific studies (Jin *et al.* 2007, Demir *et al.* 2016a, Ferrotto *et al.* 2018). Consequently, a numerical investigation opportunity of the cracking behavior of RC members provides an alternative convenient way for researchers to conduct more feasible, fast and accurate research.

In the literature, there is an insufficient study on the numerical prediction of concrete crack widths. However, this subject recently takes attention among researchers along with improvement in computer technology. On the other hand, there are some empirical formulations in past design codes such as BS:8110 (1989) and ACI 318-14 (2014) to calculate maximum crack widths to control the serviceability behavior of RC members. Those expressions have been used basically for flexural beams and thus they were defined as a function of concrete cover thickness, the stress in reinforcement, and the configuration of longitudinal reinforcement, etc. However, the crack widths are defined as a function of average crack spacing and reinforcement strain as an alternative method (Chowdhury 2001, Vidal 2004). Theiner and Hofstetter (2009) applied this method to predict crack widths on RC structures as well. Similarly, this method can also be applied to conventional FE analysis to obtain crack widths numerically (Vidal 2004, Marecki *et al.* 2007, Birrcher *et al.* 2009). On the other hand, that method has some fundamental deficiencies. Namely, the determination of the crack spacing is a very difficult job since it varies under different circumstances as well (Gopinath *et al.* 2009).

An alternative technique and formulas were proposed by

*Corresponding author, Ph.D.

E-mail: aydindemir@sakarya.edu.tr

^aProfessor

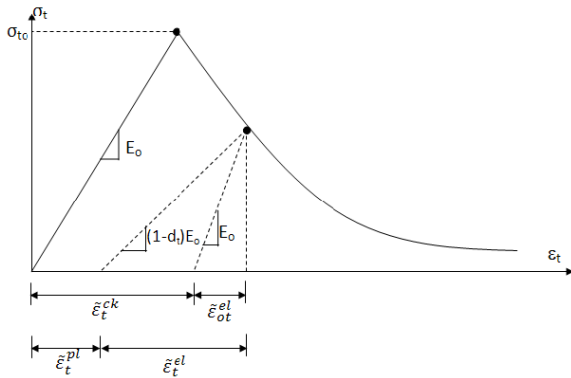


Fig. 1 Uniaxial tensile behavior of concrete (ABAQUS Documentation 2018)

Gopinath *et al.* (2009) to obtain crack widths numerically using the results of an FE model. In that method, crack widths can be calculated as a function of tension softening behavior of concrete. It comprises the conversion of strain into width in smeared models of an FE analysis. The method is based on the fact that the concrete cracks upon strains on it reach to the strain (ε_{t0}) corresponding to maximum tensile stress (σ_{t0}). Once the applied load is increased, the cracks propagate perpendicular to the direction of maximum principal tensile strains (rotating crack model). That directional relationship of crack characteristics with maximum principal tensile strains enables estimation of nonlinear behavior of different RC members after cracking. Moreover, despite the method proposed by Gopinath *et al.* (2009) appears quite practical and convenient in essence to calculate crack widths using the results of a numerical FE model, the proposed formulas have some important deficiencies. Firstly, the use of the proposed expressions is restricted to the model which was derived from the tension softening model of Petersson (1981). Therefore, it is necessary to propose new expressions for any other tension softening models given in the literature, and their accuracy must be checked. It is apparent that this process is not feasible because it requires conducting new additional experimental and numerical studies needing a high amount of budget, time and labor. Secondly, in the related study (Gopinath *et al.* 2009), the accuracy of the proposed method has not been verified sufficiently. Therefore, it requires more additional experimental studies to check its reliability.

On the other hand, Liu *et al.* (2018) developed a numerical model to calculate the crack width in RC beams depending on the bond-slip theory. The proposed model was verified using experimental data, and the results were compared to some code formulas. Consequently, the results obtained from code formulas found to be more conservative. Additionally, Yang *et al.* (2018) proposed a numerical method to predict crack width for concrete structures under the corrosion effect. The initiation and propagation of the cracks in concrete were simulated in a numerical formulation via a cohesive crack model for concrete. Moreover, the surface crack width was determined as a function of service time.

When the existing studies in the literature are evaluated

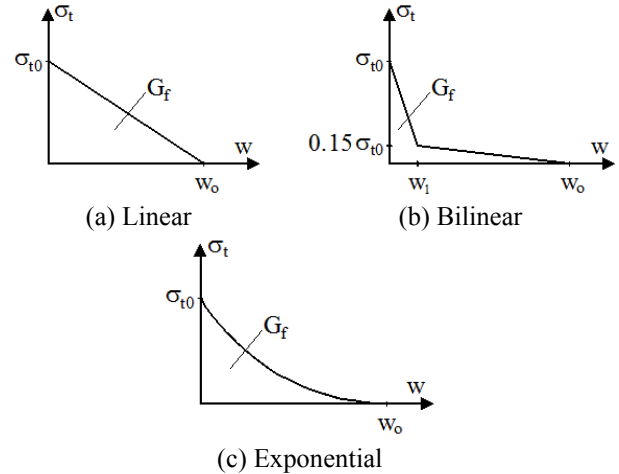


Fig. 2 Tensile behavior of concrete after cracking (Demir *et al.* 2016b)

together, it is apparent that a new general expression requires to predict crack widths numerically on an FE model irrespective of any tension softening model specified in the literature. By this means the numerical cracking and serviceability analysis of RC members can be made simpler via the FE method. Therefore, the first motivation of the present study to make a significant contribution to the literature so as to eliminate the need in the literature. For this objective, a new, simple, and alternative formula to calculate crack widths on an FE model irrespective of any specific tension softening model existing in the literature is proposed. Moreover, the second motivation of the study is to check the accuracy of the method of Gopinath *et al.* (2009) via a new experimental and numerical study. Therefore, the accuracy of the newly proposed formula and the method of Gopinath *et al.* (2009) is verified via the test results of a recent existing experimental study conducted by the authors of the present study. In the study, lastly, numerical FE models of the tested specimens are created by using an FE code ABAQUS (2018), and they are verified sufficiently according to the test results. The crack widths calculated with respect to the results of the numerical models are compared with the test results in order to see the performance of the proposed formula.

2. Determination of crack widths on a nonlinear finite element model

A typical uniaxial 'stress vs. strain behavior of concrete under tension ($\sigma_t - \varepsilon_t$)' which is characterized by damage plasticity is displayed in Fig. 1. Concrete behaves linear elastic up to maximum tensile strength (σ_{t0}). The slope of the elastic part of the curve is defined as the initial modulus of elasticity (E_0) and strains corresponding to σ_{t0} can be calculated by dividing maximum tensile strength by E_0 . Upon reaching maximum tensile strength, tensile cracks initiate on the concrete. Later on, the tensile strength of concrete drops rapidly along with the initiation and propagation of tensile cracks. As a result, a sudden and brittle behavior is observed (ABAQUS Documentation

Table 1 Dimensional and material properties of the specimens

#	Specimen ID	h [mm]	b_w [mm]	a [mm]	a/d	l_t [mm]	ρ_l	ρ_v	ρ_h	f_{ck} [MPa]
1	DB50/1.40-C1	500	200	600	1.40	1700	0.02201	0	0	18.1
2	DB50/1.86-C1	500	200	800	1.86	2100	0.02201	0	0	18.1
3	DB60/1.86-C1	600	200	1000	1.86	2500	0.02113	0	0	18.1
4	DB60/1.86-C1/SR	600	200	1000	1.86	2500	0.02113	0.00279	0.00320	18.1
5	DB40/1.86-C1	400	200	600	1.86	1700	0.02348	0	0	18.1
6	DB40/1.86-C2	400	200	600	1.86	1700	0.02348	0	0	25.3

2018). This behavior of concrete is defined as a softening ‘stress vs. strain’ response including strain localization. The tension softening response of concrete can generally be defined numerically by a smeared crack model approach. In this model, the cracks are represented as parallel micro cracks smeared over finite elements. This method is very reliable and convenient to model RC members numerically due to the fact that cracks are defined as a function of material properties. It allows the cracks to propagate in any orientation as well (Karayannis 2000, Cerioni *et al.* 2008). Moreover, the tensile behavior of concrete after peak stress can generally be defined as linear, bilinear, or exponential forms as depicted in Fig. 2 (Demir *et al.* 2016b).

The post-failure ‘stress vs. strain’ behavior of concrete in tension is mesh sensitive (Van Mier 1986, Hillerborg 1989). Therefore, the post-peak tensile behavior of concrete should be specified in terms of ‘stress vs. crack width (w)’ to avoid that unreasonable mesh sensitivity (Hillerborg 1989, Karayannis 2000, ABAQUS Documentation 2018). Moreover, the energy requiring to form a single crack for a unit crack plane area is defined as fracture energy (G_f). The area under the curve of $\sigma_t - w$ gives the fracture energy (Fig. 2(c)) which is

$$G_f = \int_{\sigma_{t0}}^0 \sigma_t dw \quad (1)$$

considering that the average fracture strain, ε_t^{ck} , over the front of the crack band is equal to w/l_w then

$$G_f = l_w \int_{\sigma_{t0}}^0 \sigma_t d\varepsilon_t^{ck} \quad (2)$$

where, l_w , the width of the fracture process zone (representative length) corresponding to mesh size in the FE method. The total strain; ε_t is defined as the sum of the elastic strain (ε_{t0}^{el}) with respect to the undamaged material where $\varepsilon_{t0}^{el} = \sigma_{t0}/E_0$ and fracture (inelastic) strain components (ε_t^{ck}) (Eq. (3)) (Birtel and Mark 2006, Alfarah *et al.* 2017).

$$\varepsilon_t = \varepsilon_{t0}^{el} + \varepsilon_t^{ck} = \frac{\sigma_{t0}}{E_0} + \frac{w}{l_w} \quad (3)$$

The unloading response of concrete is weakened upon a specimen is unloaded from any point on the strain-softening branch of the $\sigma_t - \varepsilon_t$ curves. The degradation of the elastic stiffness is characterized by a damage variable, d_t which is assumed to be functions of plastic strains (ε_t^{pl}). The damage variable can take values from zero to one, the former represents the undamaged material and the latter

corresponds to the total loss of strength (Sena Cruz *et al.* 2006, ABAQUS Documentation 2018). Eventually, tensile stresses can be calculated by using Eq. (4). Moreover, ε_t^{pl} refers to principal tensile plastic strains and controls the evolution of the failure mechanism. The cracking strains can be converted to plastic strains using the relationship given in Eq. (5) (ABAQUS Documentation 2018).

$$\sigma_t = (1 - d_t)E_0(\varepsilon_t - \varepsilon_t^{pl}) \quad (4)$$

$$\varepsilon_t^{pl} = \varepsilon_t^{ck} - \frac{d_t}{(1 - d_t)} \frac{\sigma_t}{E_0} \quad (5)$$

If ε_t^{ck} is substituted in Eq. (5), then Eq. (6) is obtained. If w is transferred and left alone on one side of Eq. (6), the expression for crack width is derived as given in Eq. (7).

$$\varepsilon_t^{pl} = \frac{w}{l_w} - \frac{d_t}{(1 - d_t)} \frac{\sigma_t}{E_0} \quad (6)$$

$$w = \left[\varepsilon_t^{pl} + \frac{\sigma_t d_t}{(1 - d_t)E_0} \right] l_w \quad (7)$$

where, ε_t^{pl} : principal tensile plastic strain obtained from an FE model, σ_t : tensile stress corresponding to ε_t^{pl} , d_t : damage parameter corresponding to σ_t , and l_w : mesh size. If tensile damage is ignored in an FE analysis, ε_t^{pl} becomes equal to ε_t^{ck} (Sena Cruz *et al.* 2006, ABAQUS Documentation 2018). Therefore, crack widths can be calculated by using Eq. (8). Nevertheless, it should be noted that Eq. (7) can give more sensitive and accurate results than Eq. (8) as well.

$$w = \varepsilon_t^{ck} \cdot l_w \quad (8)$$

Consequently, the crack widths can be calculated by reading principal tensile strain values on an element at the desired step on an FE model, and by using the proposed formula (Eq. (7) or Eq. (8)). In every step of an analysis, a curve of ‘load vs. crack width ($P - w$)’ can be constituted by a combination of applied load and crack width values calculated by using one of the proposed expressions.

The proposed crack width formula (Eq. (7)) has very significant advantages over those available in the literature. Namely, it does not rely on an estimate of average crack spacing which is very difficult to determine and has no physical meaning. Alternatively, the strains computed from a conventional nonlinear finite element analysis are directly used to calculate the crack width numerically. Since the strains are predicted in an FE analysis by accounting for a variety of geometry, loading and material conditions, the

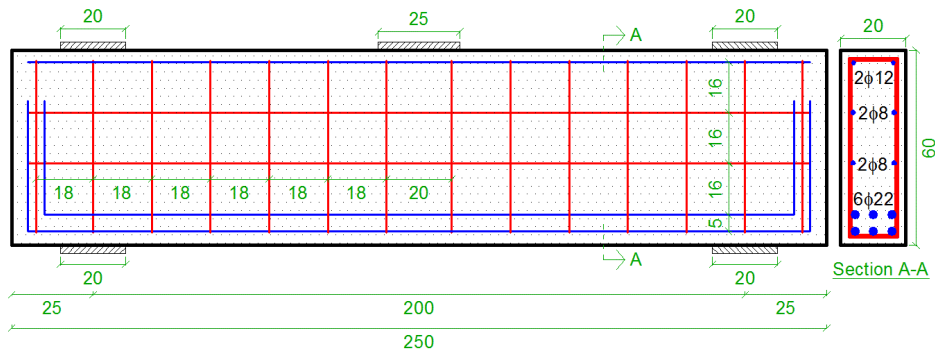


Fig. 3 Detailed drawings of DB60/1.86-C1/SR specimen (units in cm) (Demir *et al.* 2019)

derived expression is considered to be more general in nature. Moreover, the use of the proposed expression is not restricted to any constitutive tensile material model. Therefore, any concrete tension softening model in the literature can be used conveniently with the proposed formula during calculations.

On the other hand, since the proposed formula depends on the conversion of the strain into width via a representative length which is the mesh size of an FE model, an accurate determination of the mesh size is the most important issue in this method. Once 2D plane or 3D solid elements are used for concrete in an FE model, the aspect ratio of the elements should be selected properly as meshing the concrete. In the literature, the selection of the aspect ratio of the elements as 1 with equal dimensions has been proposed as the most appropriate way to eliminate numerical deficiencies (Birtel and Mark 2006, Demir *et al.* 2016b). Moreover, a parametric sensitivity analysis should be conducted to determine the optimum mesh size of the FE models because no certain mesh size has been proposed in the literature.

3. Experimental study

A recent existing experimental study of the authors (Demir *et al.* 2019) is selected as a reference study so as to verify the accuracy of the method and proposed formula to predict numerically crack widths on an FE model. The results of six RC deep beam specimens having different section heights (h), the ratio of shear span to effective depth (a/d) and compressive strength of concrete (f_{ck}) are chosen from the reference study. The selected specimens were designed according to the requirements given in ACI 318-14 (2014) code, and some of them do not contain any shear reinforcement in their shear zones. The dimensional and material properties of the selected specimens are given in Table 1. In the table, f_{ck} , b_w , l_t , ρ_l , ρ_v , and ρ_h represent 28-day characteristic cylindrical compressive strength of concrete, section width, the total length of the specimen, the ratio of tension, stirrup, and horizontal web reinforcement respectively. Moreover, a detailed drawing of the geometry and reinforcing details of DB60/1.86-C1/SR specimen is shown in Fig. 3 as a sample.

The produced RC deep beam specimens were tested under a 3-point loading condition with a pinned and a roller

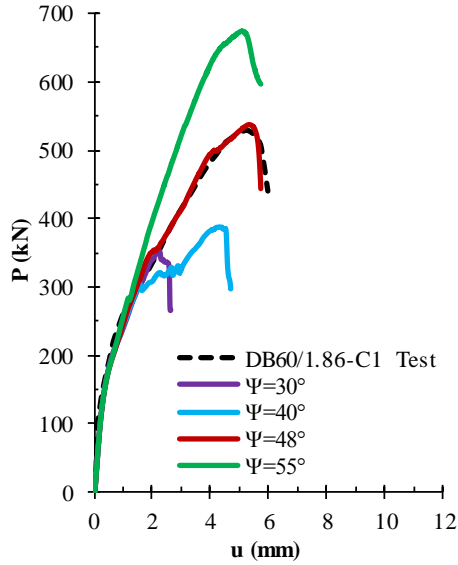
Table 2 Results of the material tests (Demir *et al.* 2019)

Strength type of concrete	Average maximum compressive strength	Diameter of reinforcement	Average yield strength
C1	18.1 MPa	Ø8 ve Ø12	421 MPa
C2	25.3 MPa	Ø18 Ø22	454 MPa 482 MPa

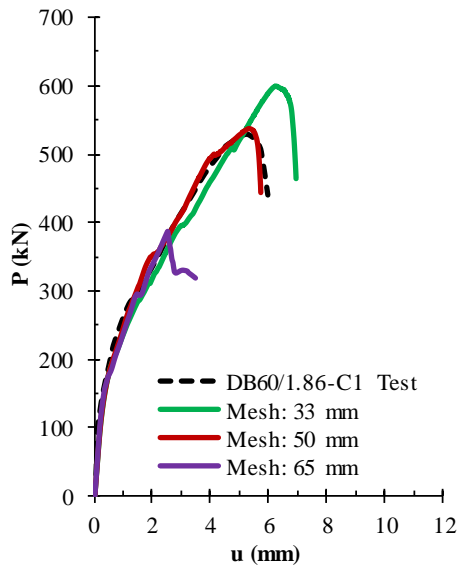
support. During tests, a quasi-static monotonic loading was applied manually to the specimens via a hydraulic cylinder. The applied load was measured via a load cell placed between the hydraulic cylinder and specimens. Vertical displacements occurring bottom of specimens were measured by linear potentiometers. Two linear crack gauges are placed on the back surface of the specimens to measure diagonal crack widths (Demir *et al.* 2019). Moreover, the reported compressive strength of concrete and yield strength of reinforcement are given in Table 2. The explanation of the naming convention and further details about the specimens and tests can be found in the reference study.

4. Numerical study

In the study, numerical simulations are carried out via an FE code ABAQUS (2018) which can simulate a wide range of linear and nonlinear problems. ABAQUS is a widely preferred software to solve many civil engineering problems by researchers as well (Khennane 2013, Panto *et al.* 2017, Ozturk *et al.* 2019, Liu and Bai 2019). In the FE models, instead of considering the restraint effect of stirrups in the constitutive equation of concrete, concrete and steel bars are modeled as separate parts. Later, the interaction between them is defined in the models with a full interaction assumption. Therefore, concrete and steel bars are simulated as a 3-dimensional (3D) solid and a truss part respectively. The reinforcement is assumed as fully embedded into the concrete as well. Thus, the confinement effect of reinforcement is ensured numerically in the models (Demir *et al.* 2016b, Ferrotto *et al.* 2018, Kaya and Yaman 2018). Accordingly, an 8-node linear 3D brick (C3D8R) and a 2-node linear 3D truss (T3D2) are used as element types from the ABAQUS element library. Later on, load and support plates are modeled as analytically rigid elements to simplify nonlinear equations to improve the convergence



(a) For dilation angle



(b) For mesh

Fig. 4 The sensitivity analysis results of DB60/1.86-C1 specimen

performance of the models. A tie constraint representing full contact interaction is assigned to surfaces between concrete and steel plate elements. A pin and a roller restraint are defined on the support plates similar to the test setup. The load is applied as a displacement-based procedure on the loading plate.

The nonlinear material behavior of concrete is defined by using concrete damage plasticity (CDP) model which is a built-in material model in ABAQUS. CDP can be used conveniently to model concrete and other quasi-brittle materials since it considers the isotropic damaged elasticity concept with isotropic tensile and compressive plasticity. Moreover, it takes into account the degradation of the elastic stiffness induced by plastic straining both in tension and compression. A viscoplastic regularization is applied to the FE model by defining a small value of viscosity parameter (μ) as 0.0001 to improve the convergence

Table 3 The values used to constitute the CDP material model in ABAQUS.

Parameter	Value
μ	0.0001
ϵ	0.10
σ_{b0}/σ_{c0}	1.16
K	0.667

Table 4 The parameters used to create the constitutive material models

σ_{cu} [MPa]	σ_{cm} [MPa]	ϵ_{c1}	E_{c1} [MPa]	E_{c0} [MPa]	α_E	E_0 [MPa]	b_c	G_{cl} [N/mm]
18.1	26.1	0.00205	12750	21500	1	25398	0.5	20
25.3	33.3	0.00220	14900			28008		25

performance of the FE models. The necessary values required to constitute the CDP material model in ABAQUS are defined by considering default values recommended in the literature. Therefore, the eccentricity (ϵ), the ratio of initial equibiaxial compressive yield stress to initial uniaxial compressive yield stress (σ_{b0}/σ_{c0}), and the ratio of the second stress invariant on the tensile meridian (K) are taken as 0.10, 1.16, and 0.667 respectively (ABAQUS Documentation 2018). Additionally, as an optimum value of dilation angle (Ψ), representing the volumetric change in brittle materials, the values around 50-degree have been proposed in the literature for RC deep beams (Demir *et al.* 2016a, Demir 2017). Therefore, a parametric study is performed to determine the most accurate values of dilation angles. As a result, 48-degree is determined as an optimum value for the dilation angle of the FE models in the present study. Results of the sensitivity analysis of dilation angle for the DB60/1.86-C1 specimen are given in Fig. 4 as a sample.

Additionally, a parametric sensitivity analysis is conducted to determine the optimum mesh size of the models by using the mesh sizes of 20, 33, 50 and 65 mm with an aspect ratio of 1. The results of the parametric study performed for the specimen of DB60/1.86-C1 are demonstrated in Fig. 4. The analysis result of the numerical model with a 20 mm mesh size is not shown in the figure because the analysis cannot be completed due to abortion of the job which may stem from the model having a very small mesh size. As a result of the sensitivity analysis, the optimum mesh size is determined as 50 mm for all models, and both concrete and steel bars are meshed accordingly. Lastly, the values used to constitute the CDP material model during parametric studies to determine dilation angle and mesh size in ABAQUS are summarized in Table 3. Moreover, a meshed FE model of a specimen is depicted in Fig. 5 as a sample.

A typical uniaxial 'stress vs. strain behavior of concrete under compression ($\sigma_c - \epsilon_c$)' is depicted in Fig. 6. The compressive behavior of concrete until the maximum compressive stress of concrete (σ_{cu}) is calculated by using the unconfined concrete model of FIB MC2010 (2013) model code. Here, concrete behaves linearly elastic up to σ_{c0} , and σ_{c0} can be calculated as $0.4\sigma_{cu}$. The slope of the elastic part of the curve is defined as the initial modulus of

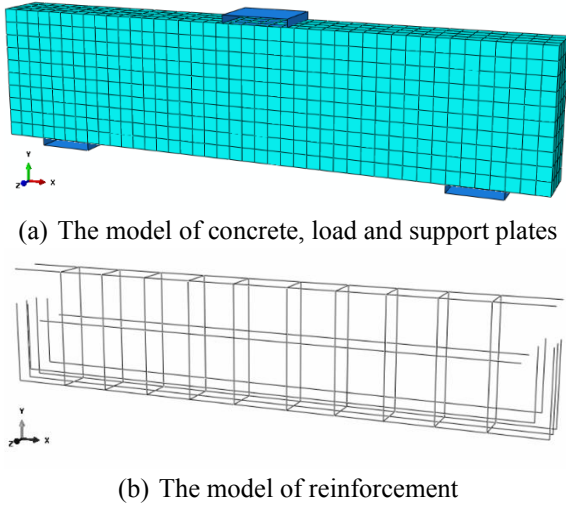


Fig. 5 A sample meshed FE model of a specimen

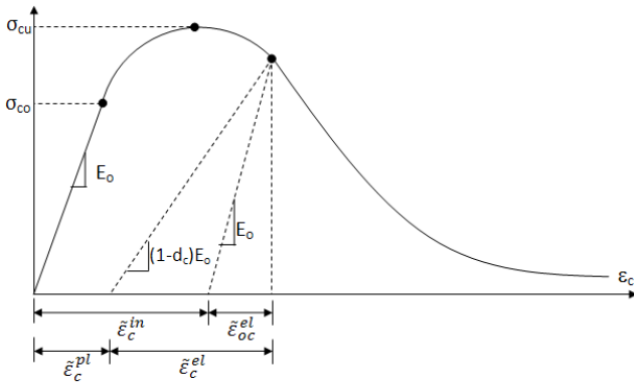


Fig. 6 Uniaxial compressive behavior of concrete (ABAQUS Documentation 2018)

elasticity (E_0), and the strain corresponding to σ_{c0} can be calculated by dividing σ_{c0} by E_0 . Moreover, the maximum compressive stress of concrete is determined via material tests reported previously in Table 2. The behavior of concrete between σ_{c0} and σ_{cu} is calculated according to the expression defined in FIB MC2010 (2013) as given in Eq. (9).

$$\sigma_c = \sigma_{cm} \left(\frac{k \cdot \eta - \eta^2}{1 + (k - 2)\eta} \right) \quad (9)$$

where, $\sigma_{cm} = \sigma_{cu} + 8$ in MPa, $\eta = \varepsilon_c / \varepsilon_{c1}$, and $k = E_{ci} / E_{c1}$. Here, E_{ci} can be calculated via Eq. (10). The parameters of ε_{c1} , E_{c1} , E_{c0} , and α_E are selected from the tables defined in FIB MC2010 (2013) depending on the grade of concrete used in the study. Moreover, E_0 equals to $\alpha_i \cdot E_{ci}$, and α_i can be calculated by using Eq. (11).

$$E_{ci} = E_{c0} \cdot \alpha_E (\sigma_{cm} / 10)^{1/3} \quad (10)$$

$$\alpha_i = 0.8 + 0.2(\sigma_{cm} / 88) \leq 1.0 \quad (11)$$

Additionally, the post-peak compressive response of concrete is determined via the post-peak compression model of Vonk (1993). This behavior is defined as in Eq. (12) and the parameter of γ_c used in that equation can be calculated via Eq. (13).

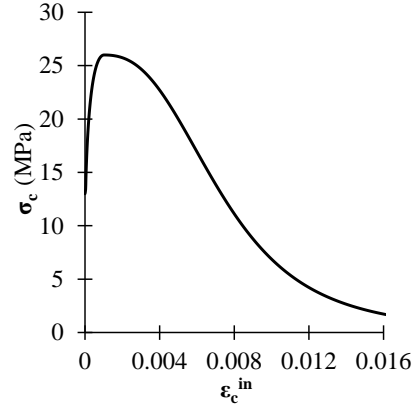


Fig. 7 The uniaxial response of concrete under compression

$$\sigma_c = \left(\frac{2 + \gamma_c \cdot \sigma_{cm} \cdot \varepsilon_{c1}}{2\sigma_{cm}} - \gamma_c \cdot \varepsilon_c + \frac{\gamma_c \cdot \varepsilon_c^2}{2 \cdot \varepsilon_{c1}} \right)^{-1} \quad (12)$$

$$\gamma_c = \frac{\pi^2 \cdot f_{cm} \cdot \varepsilon_c}{2 \left(\frac{G_{cl}}{l_w} - 0.5 \cdot \sigma_{cm} (\varepsilon_c (1 - b_c) + b_c \frac{\sigma_{cm}}{E_0}) \right)^2} \quad (13)$$

where, $b_c = \varepsilon_c^{pl} / \varepsilon_c^{in}$, and G_{cl} is the crushing energy of concrete material. Kratzig and Polling (2004) proposed as $b_c = 0.5$ and $10 \leq G_{cl} \leq 25$ in their study. Therefore, b_c is taken as 0.5, and a parametric study is performed to determine the optimum value of G_{cl} in the present study. Moreover, the parameters used in calculations to create the compressive behavior of concrete are tabulated in Table 4. On the other hand, ABAQUS enforces uniaxial compressive behavior of concrete to be assigned to a model in terms of 'stress vs. inelastic strain ($\sigma_c - \varepsilon_c^{in}$)' response. Therefore, ε_c^{in} is calculated via the equation given in Eq. (14) (ABAQUS Documentation 2018). A sample compressive material behavior of concrete assigned to the FE models is displayed in Fig. 7.

$$\varepsilon_c^{in} = \varepsilon_c - (\sigma_c / E_0) \quad (14)$$

The tensile strength of concrete (σ_{t0}) is calculated with an empirical equation (Eq. (15)) defined in FIB MC2010 (2013) by using the maximum compressive strength of concrete. Moreover, a typical uniaxial stress vs. strain behavior of concrete under tension is depicted in Fig. 1 and its details are explained above in chapter 2. The tensile behavior of concrete up to maximum stress is assumed linear elastic and determined as maximum tensile stress divided by E_0 . Moreover, the post-peak tension softening response is created by using the exponential tension softening model of Hordijk (1992). This relationship is defined in Eq. (16).

$$\sigma_{t0} = 0.3 \cdot (\sigma_{cu})^{2/3} \quad (15)$$

$$\sigma_t = \sigma_{t0} \left[\left(1 + \left(c_1 \frac{w}{w_0} \right)^3 \right) e^{-c_2 \cdot w / w_c} - \frac{w}{w_0} (1 + c_1^3) e^{-c_2} \right] \quad (16)$$

here, c_1 and c_2 are defined as constant values as 3.0 and 6.93 respectively. The maximum crack width (w_0) can be calculated as $5.14 \cdot G_f / \sigma_{t0}$. Fracture energy of concrete (G_f)

Table 5 The parameters used to create the tensile constitutive material models

σ_{cu} [MPa]	σ_{t0} [MPa]	G_f [MPa]	b_t	Poisson's ratio
18.1	2.06	0.131	0.1	0.221
25.3	2.56	0.137	0.3	0.260

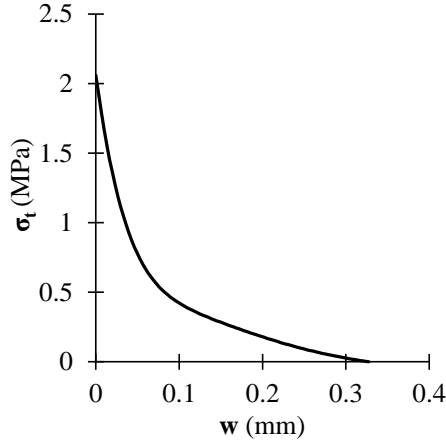


Fig. 8 The uniaxial response of concrete under tension

can be calculated according to the expression given in FIB MC2010 (2013) as in Eq. (17) as well. Moreover, the parameters used in calculations to create the tensile behavior of concrete are tabulated in Table 5. A sample tensile behavior of concrete assigned to the FE models is also depicted in Fig. 8.

$$G_f = 0.073(\sigma_{cm})^{0.18} \quad (17)$$

The damage parameters representing stiffness degradation during unloading from any point in the post-peak stress behavior of concrete for both compression (d_c) and tension (d_t) are calculated according to Eq. (18) and Eq. (19) respectively (Birtel and Mark 2006, Kamali 2012).

$$d_c = 1 - \frac{\sigma_c/E_0}{\sigma_c/E_0 + \varepsilon_c^{in}(1 - b_c)} \quad (18)$$

$$d_t = 1 - \frac{\sigma_{t0}/E_0}{\sigma_{t0}/E_0 + \varepsilon_t^{ck}(1 - b_t)} \quad (19)$$

where, b_c , ε_c^{in} , and ε_t^{ck} are previously defined above and b_t equals to $\varepsilon_t^{pl}/\varepsilon_t^{ck}$. For b_t , different values have been proposed in the literature in between 0.1 and 0.7 (Birtel and Mark 2006, Kamali 2012). Therefore, a parametric study is conducted to determine its value for different types of concrete having different compressive strengths. The acquired optimum values of them are reported in Table 5. Later, they are assigned to the FE models. Sample responses of damage parameters of concrete under compression and tension are depicted in Fig. 9 as well. Moreover, Poisson's ratio calculations are based on the equations proposed by Klink (1985), and their calculated values are given in Table 5. The further details about the definition, selection, and calculation of all parameters used to create the constitutive material model of concrete can be found in the relevant studies.

The constitutive material models of steel bars in terms

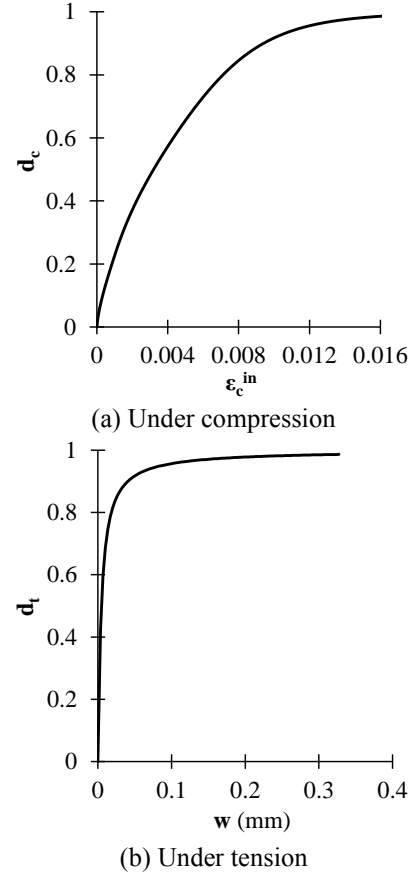


Fig. 9 Damage response of concrete

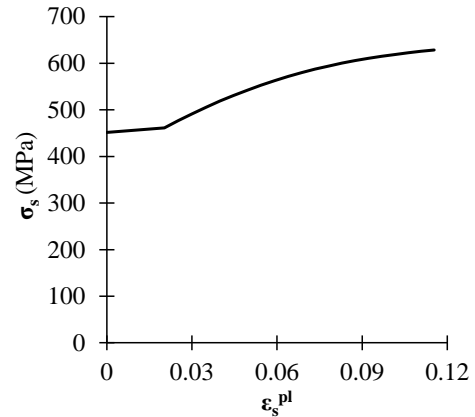


Fig. 10 A sample true stress – true plastic strain response curve of a steel bar

of 'stress vs. strain ($\sigma_s - \varepsilon_s$)' are calculated according to the reinforcement material model proposed by Mander *et al.* (1984) and later developed by Pipa (1993). The yield strength of the steel bars used in the calculation is determined experimentally as given above in Table 2. The strain hardening properties of the steel bars are also taken into account. This behavior is converted later into true stress vs. true strain to consider the plastic behavior of the steel due to the change in dimension of reinforcement (Kamali 2012). The constituted material models of steel bars are defined to the FE models in terms of 'true stress vs. true plastic strains ($\sigma_s - \varepsilon_s^{pl}$)' behavior as in the form which

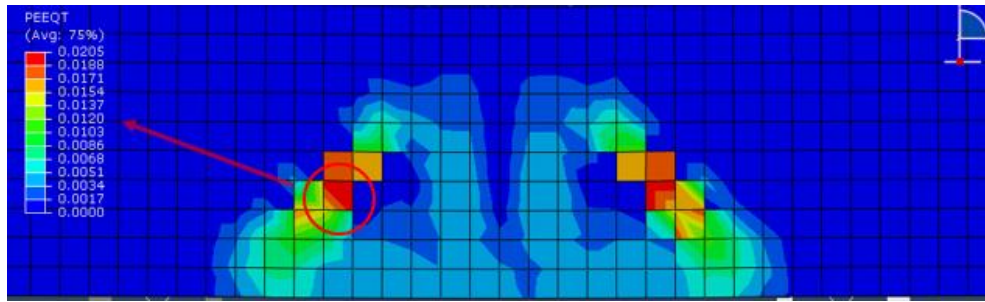


Fig. 11 The equivalent plastic strains in tension (PEEQT) on an FE model

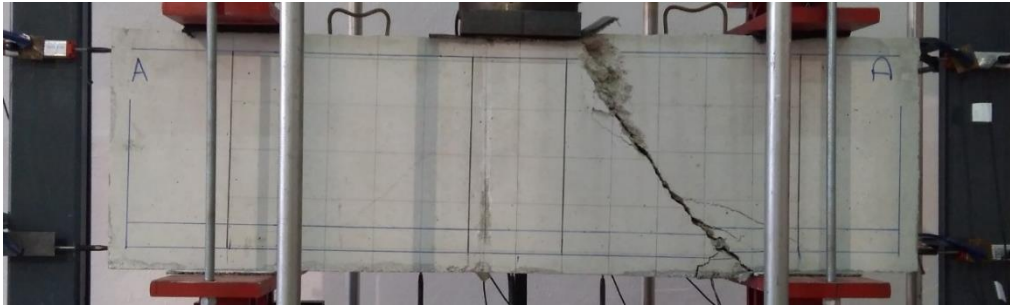


Fig. 12 The failure mode of the specimen after the tests

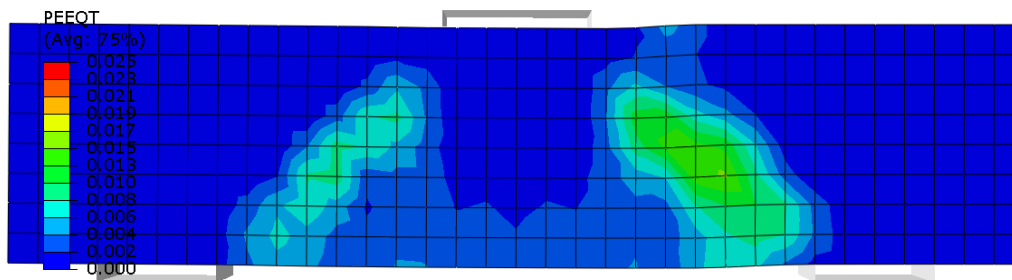


Fig. 13 Tensile damage distribution of the specimen on its FE model

ABAQUS enforces. A sample $\sigma_s - \varepsilon_s^{pl}$ response curve of a steel bar assigned to the FE models is demonstrated in Fig. 10.

After completion of the FE models, they are verified with test results in terms of their 'load vs. mid-displacement' responses. Upon sufficient convergence is successfully achieved in between test and numerical results, $P - w$ curves are constituted by the proposed formula (Eq. (7)) using the strain values obtained from the numerical models. Later on, they are compared with the test results.

Additionally, the numerical result of an FE model is depicted in Fig. 11 as a sample to demonstrate the procedure of how to obtain crack widths numerically. Firstly, the principal tensile strains should be obtained from the analysis results of an FE model. This operation can be performed in ABAQUS by reading equivalent plastic strain in tension (PEEQT) values on the concrete parts (Fig. 11). The maximum crack is obtained on an element in which maximum PEEQT occurs. By selecting that related element, the time history of PEEQT values at the integration point of that element can be obtained as a curve of 'time vs. PEEQT'. Later on, crack widths can be calculated by using one of the proposed Eq. (7) or Eq. (8) depending on whether the tensile damage is considered.

5. Results and discussion

On the specimens, no crack occurrence was observed in both flexural region and shear spans up to critical cracking load (P_{cr}). Beyond that point, diagonal cracks were initiated simultaneously in both shear zones throughout strut axes. Along with an increase in the applied load, widths of diagonal cracks were increased gradually. Ultimately, a sudden and brittle shear failure was experienced on the specimens due to reaching the ultimate load-bearing capacity of struts. A similar failure mechanism was experienced on all specimens (Demir *et al.* 2019). The failure mode of DB50/1.40-C1 specimen after the test are depicted in Fig. 12 as a sample.

Results of the numerical models verified according to their corresponding test results in terms of 'load vs. mid-displacement ($P - u$)' behavior are demonstrated between Figs. 14-16. In the figures, the letters of 'T' and 'N' at the end of specimen names designate the words of 'test' and 'numerical' respectively. It is apparent from the graphs that the results of numerical models match very well with the results of the tested specimens. Moreover, the numerical tensile damage distribution of the specimen, whose failure mode after the test is depicted above in Fig. 12, is shown in

Table 6 The test and numerical results of the specimens

Name of Specimen	Experimental				Numerical				Ratio of errors			
	P_{cr} [kN]	P_u [kN]	u_u [mm]	w_0 [mm]	P_{cr} [kN]	P_u [kN]	u_u [mm]	w_0 [mm]	P_{cr}	P_u	u_u	w_0
DB50/1.40-C1	270	645	3.82	0.57	285	645	3.44	0.54	0.95	1.00	1.11	1.06
DB50/1.86-C1	240	500	4.71	0.94	255	504	4.72	0.95	0.94	0.99	1.00	0.99
DB60/1.86-C1	235	529	5.22	0.96	230	538	5.32	0.87	1.02	0.98	0.98	1.10
DB60/1.86-C1/SR	245	664	5.06	0.92	245	650	5.72	0.82	1.00	1.02	0.88	1.12
DB40/1.86-C1	200	459	4.56	0.88	195	460	4.43	0.88	1.03	1.00	1.03	1.00
DB40/1.86-C2	215	529	4.06	0.78	190	525	4.50	0.57	1.13	1.01	0.90	1.37

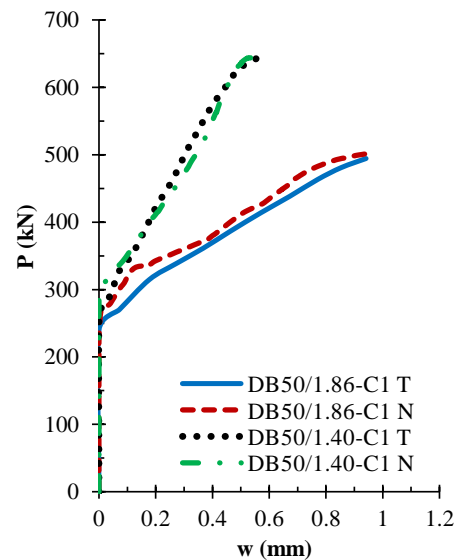
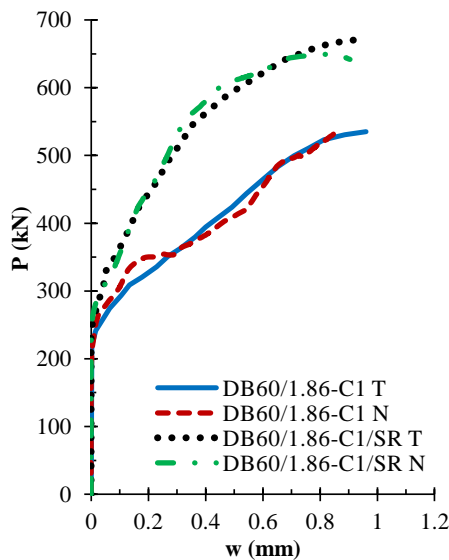
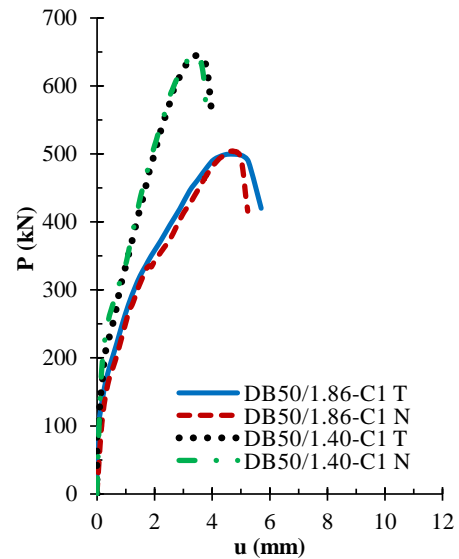
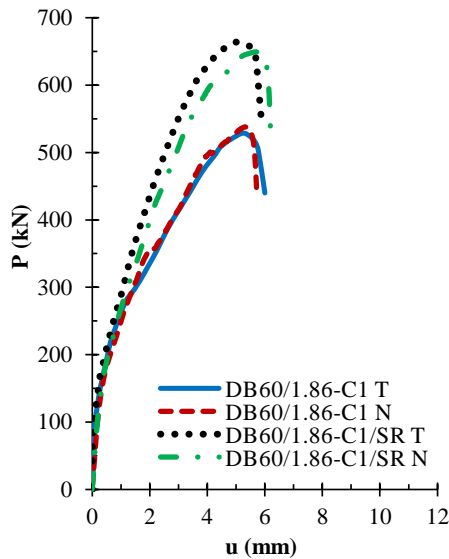


Fig. 14 Comparison of the test and numerical results for DB60/1.86-C1 and DB60/1.86-C1/SR specimens

Fig. 15 Comparison of the test and numerical results for DB50/1.86-C1 and DB50/1.40-C1 specimens

Fig. 13 as a sample. A very similar behavior is also observed in another specimens. It can be seen clearly from the figure that stress concentrations are observed between loading and support plates in the directions of diagonal cracks as experienced in the test. Ultimately, it can be deduced from the results that numerical models are highly successful and accurate to represent the nonlinear behavior of the tested specimens.

Moreover, as stated above, the specimens represent a sudden reduction in their load capacities due to shear failure during the tests. Therefore, the falling parts of $P - u$ curves are shown in the relevant figures to show this behavior. However, diagonal crack widths of the specimens increase dramatically and reach very high values beyond the point the specimens reach their ultimate load-bearing capacities. In other words, no decrease is observed in crack

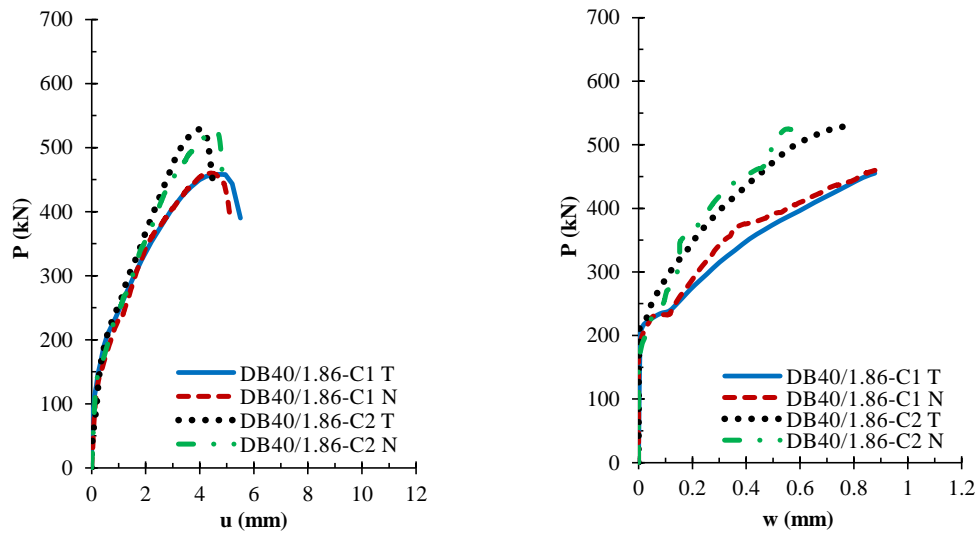


Fig. 16 Comparison of the test and numerical results for DB40/1.86-C1 and DB40/1.86-C2 specimens

width measurements, and very large crack widths are obtained experimentally. Therefore, crack width measurements after maximum load capacity (P_u) is reached, do not give meaningful result since the specimens exceed their capacities and fail rapidly. Because of this reason, the rest of the $P - w$ curves after the ultimate load capacity of the specimens are cut and not shown throughout in Figs. 14-16.

Later, the diagonal crack widths are calculated by the proposed expression (Eq. (7)) using PEEQT results obtained from the numerical models. They are compared with the test results, and the comparisons are depicted in between Figs. 14-16. It can be seen from the graphs that the proposed formula gives very accurate results in a comparison with the test results of RC deep beams having different h , a/d , and f_{ck} . Similarly, a very successful match is also observed on the specimen including shear reinforcement (Fig. 14).

Finally, the test and numerical results of the specimens in terms of critical cracking load (P_{cr}), maximum load capacity (P_u), corresponding maximum displacement (u_u), and maximum crack width at ultimate load (w_0) are reported in Table 6. In the table, the ratios of errors calculated according to the division of the test results with the numerical results are given as well. It is clear in the table that the ratios of errors stay commonly at an acceptable level. They similarly show that the numerical models are highly successful to represent the nonlinear response of RC deep beams. The maximum crack width values calculated by using the proposed expression match very well with the test results as well. However, while the general numerical cracking behavior of the numerical model of DB40/1.86-C2 specimen matches very well with its conjugate test specimen in terms of $P - u$ response, a minor difference (37 %) has occurred in the maximum crack width results (Fig. 16). Since the maximum crack width is very low around 0.78 mm on that specimen, it is thought that this difference may stem from an unexpected deviation that occurred on the measurement devices used to measure crack widths.

6. Conclusions

In the study, a new, simple, and alternative expression is proposed to calculate crack widths of concrete on an FE model. By considering a more general tension softening behavior of concrete, the proposed formula is derived irrespective of any tension softening model which is given in literature or design codes. Moreover, the test results of six RC deep beam specimens having different geometrical and material properties selected from a recent existing study are used to verify the accuracy and reliability of the proposed formula. Consequently, the following conclusions are deduced from the study:

- The results of the numerical simulations show that numerical models are highly successful to represent the nonlinear behavior of the tested specimens in terms of $P - u$ behavior.
- The proposed formula can give very accurate results in terms of diagonal crack widths in a comparison with the test results on RC deep beams having different h , a/d , and f_{ck} .
- A very successful match is also observed in crack widths on the specimen including shear reinforcement.
- The ratio of errors calculated according to the division of the test and numerical results stay commonly at an acceptable level.
- The proposed expression is quite simple, unique, and robust to determine crack widths on an FE model.
- The method, proposed in the literature and involving conversion of the strain into width in smeared models of an FE analysis, can be used conveniently for RC deep beams to predict crack widths numerically.

Lastly, the proposed formula can be conveniently used in different RC members such as columns, shear walls, etc. under different loading conditions. However, new researches are needed to determine the accuracy and performance of it on those members. Moreover, the influence of bond-slip behavior on the crack width formula should be investigated in future studies.

Acknowledgments

The study is supported by The Scientific and Technological Research Council of Turkey (TUBITAK) through Project no: 117M854.

References

- ABAQUS Documentation (2018), Dassault Systèmes, 10 rue Marcel Dassault CS 40501 78946 Vélizy-Villacoublay Cedex, SE, France.
- ABAQUS Research Edition (2018), *Abaqus unified FEA*, Dassault Systèmes, 10 rue Marcel Dassault CS 40501 78946 Vélizy-Villacoublay Cedex, SE, France.
- ACI 318-14 (2014), Building Code Requirements for Structural Concrete and Commentary, American Concrete Institute, Michigan, USA.
- Alfarah, B., López-Almansa, F. and Oller, S. (2017), "New methodology for calculating damage variables evolution in plastic damage model for RC structures", *Eng. Struct.*, **132**, 70-86. <https://doi.org/10.1016/j.engstruct.2016.11.022>.
- Bazant, Z.P. and Oh, B.H. (1983), "Crack band theory for fracture of concrete", *Mater. Constr.*, **16**, 155-177. <https://doi.org/10.1007/BF02486267>.
- Bircher, D., Tuchscherer, R., Huizinga, M., Bayrak, O., Wood, S. and Jirsa, J. (2009), "Strength and serviceability design of reinforced concrete deep beams", Research Report No. 0-5253-1, Center for Transportation Research, The University of Texas, Austin, USA.
- Birtel, V. and Mark, P. (2006), "Parameterised finite element modeling of RC beam shear failure", *ABAQUS User's Conference*, Boston, MA, USA.
- BS:8110 (1989), British Standard, Structural Use of Concrete - Part 2, British Standards Institutions, London, England.
- Cerioni, R., Iori, I., Michelini, E. and Bernardi, P. (2008), "Multi-directional modeling of crack pattern in 2D R/C members", *Eng. Fract. Mech.*, **75**(3-4), 615-628. <https://doi.org/10.1016/j.engfracmech.2007.04.012>.
- Chowdhury, S.H. (2001), "Crack width predictions of reinforced and partially prestressed concrete beams: A unified formula", *Struct. Eng. Mech. Comput.*, **1**, 327-334. <https://doi.org/10.1016/b978-008043948-8/50032-1>.
- Demir, A., Caglar, N. and Ozturk, H. (2019), "Parameters affecting diagonal cracking behavior of reinforced concrete deep beams", *Eng. Struct.*, **184**, 217-231. <https://doi.org/10.1016/j.engstruct.2019.01.090>.
- Demir, A., Caglar, N., Ozturk, H. and Sumer, Y. (2016b), "Nonlinear finite element study on the improvement of shear capacity in reinforced concrete T-Section beams by an alternative diagonal shear reinforcement", *Eng. Struct.*, **120**, 158-165. <https://doi.org/10.1016/j.engstruct.2016.04.029>.
- Demir, A., Ozturk, H. and Dok, G. (2016a), "3D numerical modeling of RC deep beam behavior by nonlinear finite element analysis", *Disast. Sci. Eng.*, **2**(1), 13-18.
- Demir, A., Ozturk, H., Bogdanovic, A., Stojmanovska, M. and Edip, K. (2017), "Sensitivity of dilation angle in numerical simulation of reinforced concrete deep beams", *Scientif. J. Civil Eng.*, **6**(1), 33-37.
- Ferrotto, M.F., Cavaleri L. and Di Trapani, F. (2018), "FE modeling of Partially Steel-Jacketed (PSJ) RC columns using CDP model", *Comput. Concrete*, **22**(2), 143-152. <https://doi.org/10.12989/cac.2018.22.2.143>.
- FIB MC2010 (2013), CEBS-FIB Model Code for Concrete Structures 2010, International Federation for Structural Concrete, Lausanne, Switzerland.
- Gopinath, S., Rajasankar, J., Iyer, N.R., Krishnamoorthy, T.S. and Lakshmanan, N. (2009), "A strain-based constitutive model for concrete under tension in nonlinear finite element analysis of RC flexural members", *Struct. Durab. Hlth. Monit.*, **5**(4), 311-335.
- Hillerborg, A. (1989), "Fracture mechanics: application to concrete", Research Report No. ACI-SP-118, American Concrete Institute, Michigan, USA.
- Hordijk, D.A. (1992), "Tensile and tensile fatigue behavior of concrete - experiments, modeling, and analyses", *Heron*, **37**(1), 3-79. <http://resolver.tudelft.nl/uuid:06985d0d-1230-4a08-924a-2553a171f08f>.
- Jin, N., Tian, Y. and Jin, X. (2007), "Numerical simulation of fracture and damage behaviour of concrete at different ages", *Comput. Concrete*, **4**(3), 221-241. <https://doi.org/10.12989/cac.2007.4.3.221>.
- Kamali, A.Z. (2012), "Shear strength of reinforced concrete beams subjected to blast loading", Ph.D. Dissertation, Department of Civil and Architectural Engineering, Royal Institute of Technology (KTH).
- Karayannis, C.G. (2000), "Smearred crack analysis for plain concrete in torsion", *J. Struct. Eng.*, ASCE, **126**(6), 638-645. [https://doi.org/10.1061/\(asce\)0733-9445\(2000\)126:6\(638\)](https://doi.org/10.1061/(asce)0733-9445(2000)126:6(638)).
- Kaya, M. and Yaman, C. (2018), "Modelling the reinforced concrete beams strengthened with GFRP against shear crack", *Comput. Concrete*, **21**(2), 127-137. <https://doi.org/10.12989/cac.2018.21.2.127>.
- Khennane, A. (2013), *Introduction to Finite Element Analysis Using MATLAB and Abaqus*, CRC Press, Florida, USA.
- Klink, S.A. (1985), "Actual poisson ratio of concrete", *ACI J.*, **82**(6), 813-817. <https://doi.org/10.14359/10392>.
- Kratzig, W.B. and Polling, R. (2004), "An elasto-plastic damage model for reinforced concrete with minimum number of material parameters", *Comput. Struct.*, **82**(15-16), 1201-1215. <https://doi.org/10.1016/j.compstruc.2004.03.002>.
- Liu, B. and Bai, G.L. (2019), "Finite element modeling of bond-slip performance of section steel reinforced concrete", *Comput. Concrete*, **24**(3), 237-247. <https://doi.org/10.12989/cac.2019.24.3.237>.
- Liu, J., Jia, Y., Zhang, G. and Wang, J. (2018), "Numerical calculation of crack width in prestressed concrete beams with bond-slip effect", *Multidisc. Model. Mater. Struct.*, **15**(2), 523-536. <https://doi.org/10.1108/mmms-01-2018-0008>.
- Mander, J.B., Priestley, M.J.N. and Park, R. (1984), "Seismic design of bridge piers", Research Rep. No. 84-2, Dept. of Civil Engineering, Univ. of Canterbury, Christchurch, New Zealand.
- Marecki, T., Marzec, I., Bobiski, J. and Tejchman, J. (2007), "Effect of a characteristic length on crack spacing in a reinforced concrete bar under tension", *Mech. Res. Commun.*, **34**(5-6), 460-465. <https://doi.org/10.1016/j.mechrescom.2007.04.002>.
- Ozturk, H., Caglar, N. and Demir, A. (2019), "Effectiveness of diagonal shear reinforcement on reinforced concrete short beams", *Earthq. Struct.*, **17**(5), 501-510. <https://doi.org/10.12989/eas.2019.17.5.501>.
- Panto, B., Giresini, L., Sassu, M. and Calio, I. (2017), "Non-linear modeling of masonry churches through a discrete macro-element approach", *Earthq. Struct.*, **12**(2), 223-236. <https://doi.org/10.12989/eas.2017.12.2.223>.
- Petersson, P.E. (1981), "Crack growth and development of fracture zones in plain concrete and similar materials", Research Report No. TVBM-1006, Division of Building Materials, Lund Institute of Technology, Lund, Sweden.
- Pipa, J.A.L. (1993), "Ductility of Reinforced Concrete Elements Subjected to Cyclical Actions, Influence of the Mechanical Characteristics of the Rebar", Ph.D. Dissertation, Instituto Superior Técnico, Universidade Técnica de Lisboa.
- Rots, J.G. (1988), "Computational modeling of concrete fracture", Sena Cruz, J., Barros, J. and Azevedo, A. (2006), "Elasto-plastic

- multi-fixed smeared crack model for concrete”, Research Report No. 04/DEC/E-05, Universidade do Minho, Portugal.
- Theiner, Y. and Hofstetter, G. (2009), “Numerical prediction of crack propagation and crack widths in concrete structures”, *Eng. Struct.*, **31**(8), 1832-1840. <https://doi.org/10.1016/j.engstruct.2009.02.041>.
- Van Mier, J.G.M. (1986), “Multiaxial strain-softening of concrete”, *Mater. Struct.*, **19**, 179-200. <https://doi.org/10.1007/bf02472034>.
- Vecchio, F.J. and Collins, M.P. (1986), “The modified compression field theory for RC elements subjected to shear”, *J. ACI*, **83**(6), 925-933.
- Vidal, T., Castel, A. and Francois, R. (2004), “Analyzing crack width to predict corrosion in reinforced concrete”, *Cement Concrete Res.*, **34**(1), 165-174. [https://doi.org/10.1016/s0008-8846\(03\)00246-1](https://doi.org/10.1016/s0008-8846(03)00246-1).
- Vonk, R.A. (1993), “A micromechanical investigation of softening of concrete loaded in compression”, *Heron*, **38**(3), 3-94.
- Yang, S.T., Li, K.F. and Li, C.Q. (2018), “Numerical determination of concrete crack width for corrosion-affected concrete structures”, *Comput. Struct.*, **207**, 75-82. <https://doi.org/10.1016/j.compstruc.2017.07.016>.